ASTFE
American Society
of Thermal and Fluids Engineers

8th Thermal and Fluids Engineering Conference (TFEC)
May, 2023
Partially Online Virtual and at University of Maryland, MD Conference

TFEC-2023-xxxxx

PERFORMANCE EVALUATION OF GRAY-BOX AND MACHINE LEARNING MODELS OF A THERMAL ENERGY STORAGE SYSTEM WITH ACTIVE INSULATION

Borui Cui*, Jin Dong, Piljae Im, Sungkyun Jung, Melissa Voss Lapsa

[1]Energy System Integration & Controls Section, Oak Ridge National Laboratory, USA

ABSTRACT

An interior partition wall integrated with active thermal storage and a dynamic insulation system was built and then installed in an office building in Oak Ridge, Tennessee, TN. This smart wall, termed the Empower Wall, was equipped with embedded pipes in the building envelope core component and an additional pipe network enclosing rigid insulation to switch on and off the active insulation dynamically. The performance of the wall's contribution to cooling load reduction under different parameters has been investigated in previous publications. Aiming to be deployed into model predictive control and other optimization methods, simplified and reliable models for the developed wall and the room accommodating it are required. They are needed to characterize the properties and thermal response of both Empower Wall and building envelope, which form an essential component for accurate indoor temperature or cooling/heating demand prediction. In this study, simplified gray-box and regression models as well as machine learning model were developed and the performance of them were compared and analyzed.

KEY WORDS: Thermal energy storage system, Active insulation system, Gray-box modeling, Machine learning algorithm

1. INTRODUCTION

Buildings in the United States consume about 76% of the total national electricity demand and HVAC systems are responsible for about 35% of the total energy used in residential and commercial buildings [1]. Reducing the energy consumption and peak demand of buildings is a critical step towards achieving sustainable energy demands, both nationally and internationally. Applications of building envelope systems as thermal batteries to store energy and on-demand releasing the accumulated energy can offer an opportunity to harvest thermal energy, such as during non-peak load hours. Conversely, the stored energy can be used during high peak load periods [1].

Thermally activated building systems (TABS), a well-known active thermal energy storage (TES) system in buildings, can serve as a short-term, sensible and low-temperature thermal energy storage technology by being actively charged and passively discharged [2]. These wall systems consist of pipes or ducts embedded into the building walls and are used to reduce the energy consumption required for space heating and cooling. To add an active energy discharging component, active insulation systems (AIS) can be incorporated into wall systems to release the stored energy to the indoor environment when needed. Simulation results have shown that notable energy and peak demand savings were achieved in building envelope equipped with AISs under optimal control [3]. Not many research works focus on building systems with both active storage and active discharging mechanisms. An advanced TES system integrated with an active insulation system (AIS), called *Empower Wall*, has been proposed [2,4,5]. The detailed thermal performance under different AIS/TES parameters was investigated as well as the mathematical modeling and validation results were shown in [2].

*Corresponding Author: cuib@ornl.gov

The built empower wall was then deployed into a conference room and the energy and cost savings were achieved under smart control [4]. The peak load shift capabilities of the proposed wall in different US climate zones were also evaluated [5].

Instead of detailed physical modeling methods, data-driven models, like gray-box and black-box models, are preferred in model predictive control and other optimization approaches [6]. In this paper, simplified gray-box and regression models as well as machine learning model are proposed to characterize the thermal response of the developed Empower Wall and building envelope. The performance of those models was compared and analyzed.

2. EXPERIMENT SYSTEM INTRODUCTION

2.1 Empower Wall System

An interior partition wall integrated with active thermal storage and an active (dynamic) insulation system was demonstrated in previous publications. This proposed smart wall was equipped with embedded pipes in the building envelope core component and an additional pipe network enclosing rigid insulation to dynamically switch on and off the active insulation, as shown in Fig.1.

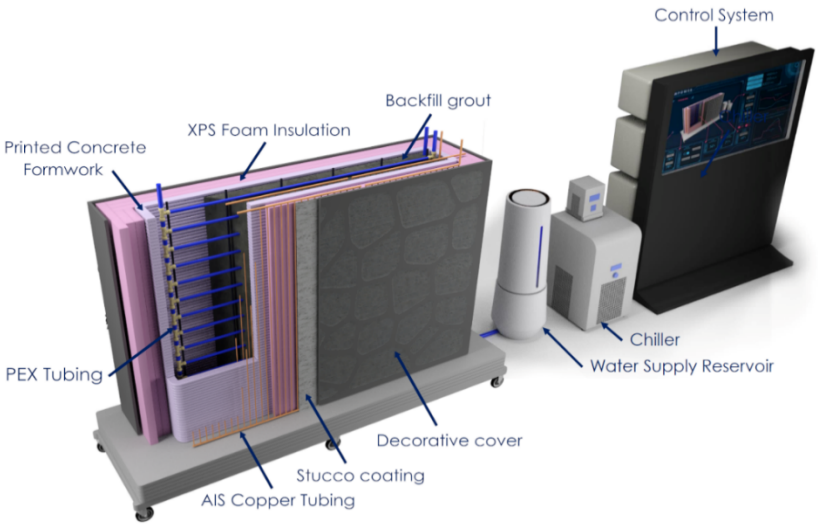

Fig. 1 Schematic layout of the EMPOWER Wall system

The two distinct pipe systems were key components that each corresponded to one of the temperature regulating systems, either the TES system or the AIS. Cross-linked polyethylene (PEX) pipes were used for the TES system, while copper pipes were used for the AIS. The wall structure was designed to be connected to a water supply reservoir, water chiller, and control system. The detailed layouts of PEX and copper piping work can be referred in [4].

All the components cooperate to regulate the temperature of the surrounding air. When cooling is needed, water is run from the external copper pipe manifold to the internal copper pipe manifold, allowing heat to be transferred from the surroundings to the thermal mass of the wall. The cool surface of the wall provides occupant comfort and reduces HVAC loads. During charging and idle times of the wall, the water circulation is shut down. The on-demand capabilities of the AIS reduce electricity costs by lowering the use of the HVAC system during peak demand hours. This capability can provide peak-load reduction, cost savings, reduced burden on the electric grid, and the higher opportunity to use renewable energy sources.

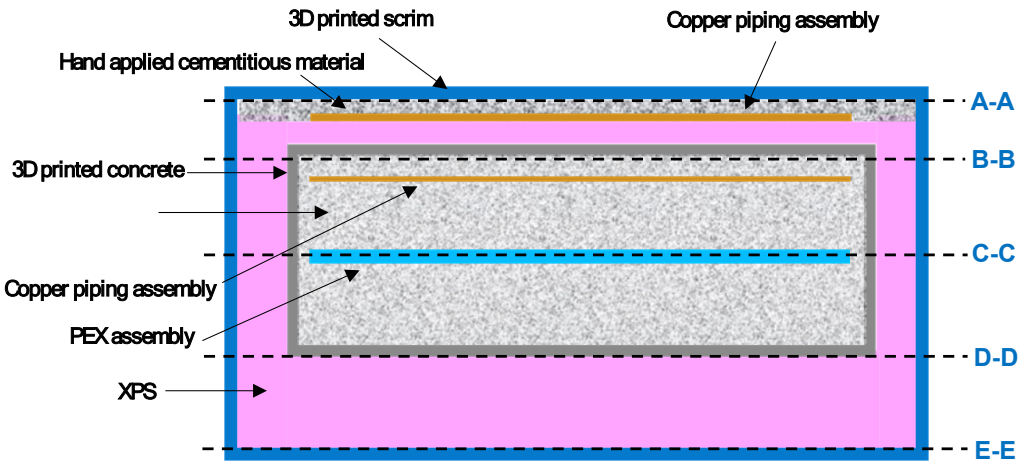

Fig. 2 Horizontal section view of Empower Wall

The horizontal section view was shown as Fig.2. The instrumented PEX tube was inserted at the central position of the concrete form in Empower Wall (at C-C plane). The concrete form, which is done by 3-D printing, was filled with grout, once the PEX tubing and the part of the copper piping were securely placed. One half component of the AIS system was placed facing one of the interior sides of the concrete form. The detailed parameters are listed in [5]. Multiple kinds of sensors, e.g., thermocouples and heat flux transducers, were on four different planes, i.e., A-A, B-B, C-C and D-D. The specifications can be also found in [5].

2.2 Test Building Information and Air Conditioning System

The reference building is an office building at Oak Ridge National Laboratory, Oak Ridge, TN, USA, as shown in Fig.3. It is an office building with 26,822 ft^2 of floor area. The building contains open office, enclosed offices, conference rooms, and shipping and receiving area. A conference room (room 102), as shown in Fig.5, was selected for deployment and demonstration of the developed Empower wall system. The room is with about 600 ft^2 (56 m^2) of conditioned floor area, and there is a dedicated roof top unit (RTU), which provides both cooling and heating for the room. The conference room is used several times per day for a meeting and other gathering purpose.

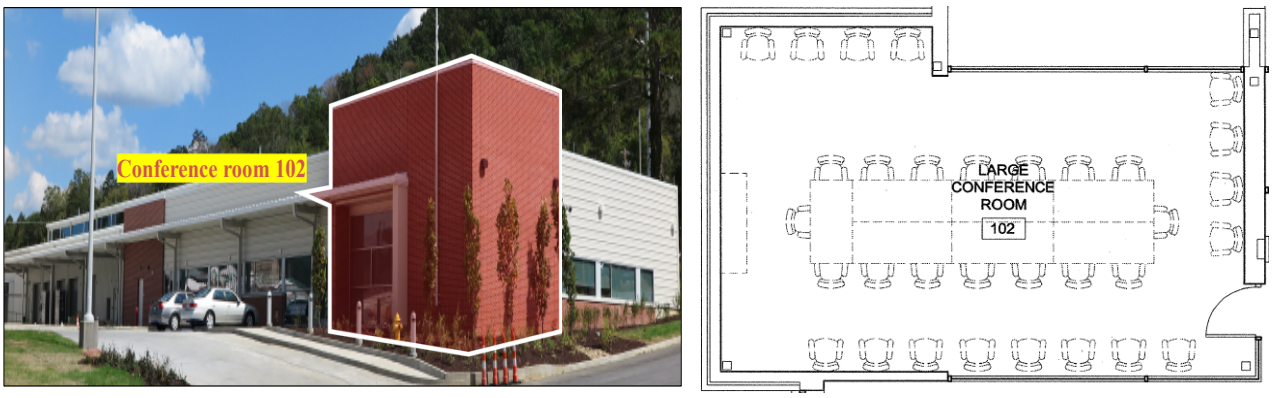

(a) reference building (b) test room

Fig. 3 View and drawing of the reference building and test room

The test period was from April 2021 to August 2021. During the test period, the Empower Wall system with RTU and RTU-only baseline system were alternately operated every other week for evaluation purposes. The

TES + AIS integrated wall system served as a secondary cooling system, and the RTU served as the primary cooling system.

3. DEVELOPMENT OF DATA-DRIVEN MODELS

This paper targets on development of data-driven models for both Empower Wall and building envelope. Those models are expected to be applied into advanced optimal control methods.

Data-driven models adopt an inverse approach for model development, assuming that there are certain mathematical relationships between model inputs and outputs [7]. Data-driven models can be further categorized into "black-box" and "gray-box" models [6]. A black-box model is purely derived from measured data, and model inputs and outputs may not necessarily present clear physical meaning. By contrast, gray-box models are built based on a combination of physical principles and measured data.

3.1 Development of gray-box model for building envelope

One of the most popular gray-box methods is the Resistance-Capacitance (RC) model, also called lumped capacitance or network model, which is composed of electrical analogue resistances (R) and capacitances (C) [8]. Capacitance represents thermal capacity (i.e., property of objects to describe its capability to store heat), while resistance represents thermal resistance (i.e., property of objects or materials to resist the heat flow through it). The values of R and C are estimated based on samples of inputs and outputs by applying an identification algorithm, e.g., nonlinear regression algorithm, which typically minimizes a norm of either simulation errors or prediction errors [9]. The boundaries on the parameters in the identification process are normally estimated from a rough description of the building geometry and materials [10]. One obvious advantage is that the RC modeling methods allow model training using short periods of data, e.g., one to four weeks, recorded by a limited number of sensors.

One simplified RC model was developed in this research to predict the mean indoor temperature, i.e., $(T_{in,left}+T_{in,right})/2$, which are measured by the two temperature sensors in the test room 102. The schematic of the developed RC model is shown in Fig. 4.

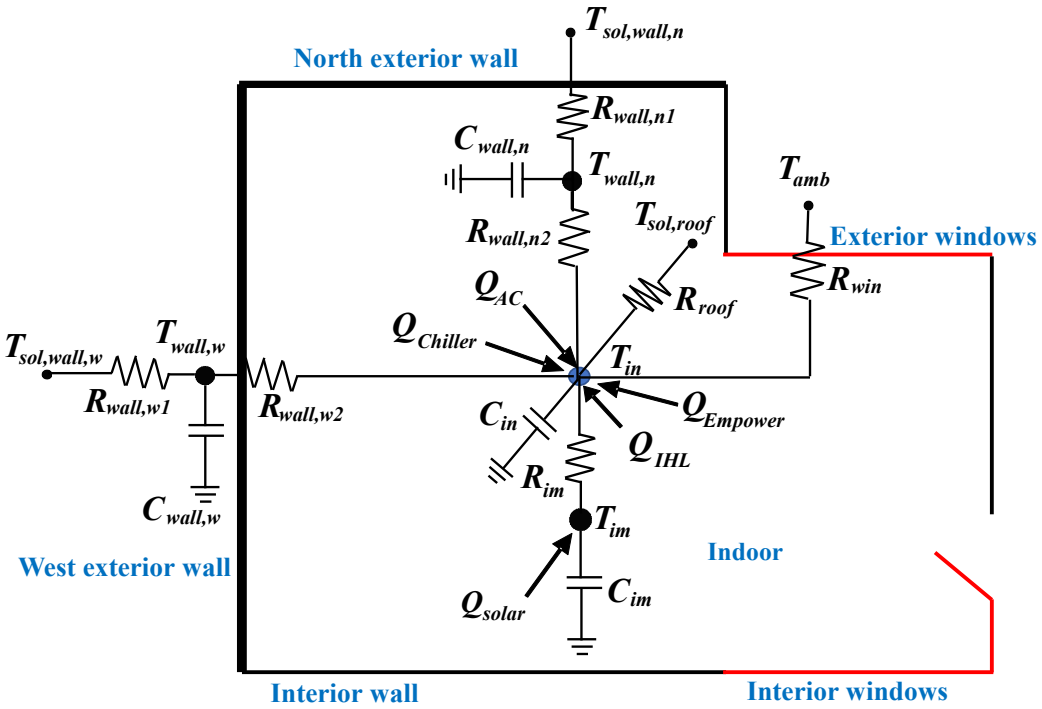

Fig. 4 Schematic of the developed building RC model

The subscript *wall, roof*, *w*, *n*, *im*, *win* and *amb* indicate exterior wall, roof, west orientation, north orientation, internal thermal mass, exterior windows and outdoor ambient temperature, respectively. Each model consists of four states: mean indoor air temperature (T_{in}), mean west exterior wall temperature ($T_{wall,w}$), mean north exterior wall temperature ($T_{wall,n}$) and mean internal thermal mass temperature (T_{im}).

The heat transfer in the building model is described using the following set of first-order differential equations:

$$C_{in}\frac{dT_{in}(t)}{dt} = \frac{T_{wall,w}(t) - T_{in}(t)}{R_{wall,w2}} + \frac{T_{wall,n}(t) - T_{in}(t)}{R_{wall,n2}} + \frac{T_{im}(t) - T_{in}(t)}{R_{im}} + \frac{T_{amb}(t) - T_{in}(t)}{R_{win}} + \frac{T_{sol,r}(t) - T_{in}(t)}{R_{roof}} + Q_{AC} * C1 + Q_{chiller} + Q_{empower} \quad (1)$$

$$C_{wall,w}\frac{dT_{wall,w}(t)}{dt} = \frac{T_{sol,w,w}(t) - T_{wall,w}(t)}{R_{wall,w1}} - \frac{T_{wall,w}(t) - T_{in}(t)}{R_{wall,w2}} \quad (2)$$

$$C_{wall,n}\frac{dT_{wall,n}(t)}{dt} = \frac{T_{sol,w,n}(t) - T_{wall,n}(t)}{R_{wall,n1}} - \frac{T_{wall,n}(t) - T_{in}(t)}{R_{wall,n2}} \quad (3)$$

$$C_{im}\frac{dT_{im}(t)}{dt} = -\frac{T_{im}(t) - T_{in}(t)}{R_{im}} + Q_{solar} * C2 \quad (4)$$

Where, T_{in} is the average of $T_{in,left}$ and $T_{in,right}$. C_{in}, $C_{wall,w}$, $C_{wall,n}$, and C_{im} are the equivalent overall thermal capacitances of indoor air, west exterior wall, north exterior wall, and internal thermal mass, respectively (J/K). $R_{wall,w}$, $R_{wall,n}$, R_{win}, R_{im}, and R_{roof} are the equivalent overall thermal resistances of west exterior wall, north exterior wall, windows, internal thermal mass, and roof, respectively (K/W).

Q_{solar} is the total solar radiation rate (W) transmitted through the exterior windows into the zone. The effects of solar radiation on exterior walls and the roof were considered by calculating $T_{sol,wall,w}$, $T_{sol,wall,n}$, and $T_{sol,roof}$ respectively, which are the sol-air temperatures.

Q_{AC} is the sensible cooling/heating supply from the HVAC (W), which is calculated from the following equation:

$$Q_{AC} = \left(T_{rtn,air}(t) - T_{sup,air}(t)\right) \cdot c_{air} \cdot \rho_{air} \cdot V_{air} \quad (5)$$

Where, $T_{sup,air}$ and $T_{rtn,air}$ are the HVAC(RTU) supply air and return air temperatures (°C), respectively. V_{air} is the volume flow rate of air (m^3/s), which is constant. ρ_{air} is the air density (kg/m^3). c_{air} is the specific heat of air (J/(kg·K)).
$Q_{chiller}$ is the heat dissipation (supplied cooling) from the empower wall chiller (W), which is calculated from the following equation:

$$Q_{chiller} = \left(T_{rtn,wa}(t) - T_{sup,wa}(t)\right) \cdot c_{wa} \cdot \rho_{wa} \cdot V_{wa} \quad (6)$$

Where, $T_{sup,wa}$ and $T_{rtn,wa}$ are the chiller supply water and return water temperatures (°C), respectively. V_{wa} is the volume flow rate of chilled water (m^3/s), which is constant. ρ_{wa} is the chilled water density (kg/m^3). c_{wa} is the specific heat of chilled water (J/(kg·K)).
$Q_{empower}$ is the discharge rate of the empower wall (W), which is calculated from the following equation:

$$Q_{empower} = HFA_{empower}(t) \cdot A_{empower} \quad (7)$$

Where, $HFA_{empower}$ is the average heat flux, which is measured by heat flux transducers, between empower A-A plane and indoor air (W/m^2). $A_{empower}$ is the empower wall area (m^2).

The solar radiation through window is characterized by Q_{solar} (W) in the following:

$$Q_{solar} = I_n(t) A_{win,tot} SHGC \quad (8)$$

where, I is the direct normal solar irradiance (W/m^2), which was measured by a dedicated weather station installed on the roof of a light commercial building which is also located closed to test building. $A_{win,tot}$ is the total exterior window area (m^2). *SHGC* is the solar heat gain coefficient of windows.

The effects of solar radiation on exterior walls (west and north walls) and the roof are considered by calculation of $T_{sol,wall,w}$, $T_{sol,wall,n,}$ and $T_{sol,roof}$ respectively, which are the sol-air temperatures, shown in the followings:

$$T_{sol,w,w}(t) = \frac{\alpha_{wall}}{h(t)} F_{wall,w}(t) I(t) + T_{amb}(t) \quad (9)$$

$$T_{sol,w,n}(t) = \frac{\alpha_{wall}}{h(t)} F_{wall,n}(t) I(t) + T_{amb}(t) \quad (10)$$

$$T_{sol,roof}(t) = \frac{\alpha_{roof}}{h(t)} F_{roof}(t) I(t) + T_{amb}(t) \quad (11)$$

where, α_{wall} *and* α_{roof} are the solar absorption coefficients of exterior wall and roof, respectively. T_{amb} is outdoor dry bulb temperature (°C), which was also measured by the weather station. $F_{wall,w}$, $F_{wall,n}$ and F_{roof} are the view factors of exterior walls and roof, which are the coefficients calculated based on the building location and season. h is convective heat transfer coefficient of roof and exterior wall surfaces (W/m^2·K). C_1 and C_2 are the effective heating/cooling gain coefficients, and they are used to adjust Q_{ac} and Q_{solar} for unknown factors. Both C1 and C2 are assumed to be unknown and need to be identified by the searching algorithm illustrated in the next sub-section.

The searching process for the optimal values of the undetermined parameters (i.e., $C_{wall,w}$, $C_{wall,n}$, C_{im}, C_{in}, $R_{wall,w1}$, $R_{wall,w2}$, $R_{wall,n1}$, $R_{wall,n2}$, R_{roof}, R_{win}, and R_{im}) in this RC models is a nonlinear optimization process. An objective function to minimize the root mean squared error (RMSE) is used to evaluate the fitness between the results predicted by the RC model and the measured data (i.e., mean indoor temperature) during the training period. The parameters were identified using the particle swarm optimization (PSO) method, which is a computational method that optimizes a problem by iteratively trying to improve a candidate solution with regard to a given measure of quality [11].

3.2 Development of simplified regression model for Empower Wall

A simplified regression model was developed to predict the discharge rate of the Empower Wall. Theoretically, the empower wall is always discharging as long as the mean wall temperature is lower than the indoor air temperature. In this research, it is assumed that no charging is conducted during in daytime, the discharging effect is considered when both chiller (for TES charging) and pump (for AIS discharging) were off only. The following equations list how the discharge rate (W) was predicted by the regression model.

For discharging period (when AIS is on):

$$Q_{empower_{simu}}(t) = Coe_{dis\_1} * \left(T_{in}(t) - Coe_{dis_2}\right) + Coe_{dis_3} * T_{C-C_{simu}}(t) + Coe_{dis_4} + Coe_{dis_5} * t^2 \quad (12)$$

Where, $Q_{empower\_simu}$ is predicted discharge rate of the empower wall (W). Coe_{dis_1}, …, Coe_{dis_5} are the coefficients. t is the time step after discharge starts (t = 0,1,2…n). $T_{C\text{-}C\_simu}$ is the predicted average temperature of C-C plane, which is calculated by the following equation:

$$T_{C-C_{simu}}(t) = Coe_{dis_6} * T_{C-C_{simu}}(t=0) + Coe_{dis_7} * t + Coe_{dis_8} \quad (13)$$

Where, Coe_{dis_6} – Coe_{dis_8} are the coefficients which are identified by least square method using historic operation data.

3.3 Development of machine learning model

In this study, a RNN (recurrent neuron network). RNN is time-series model, which recognizes the temporal structure of input data. Recurrent neural network (RNN) was shown to provide better accuracy than ANN for prediction of energy consumption [12]. In addition, compared to "shallow" machine learning algorithms, RNN is more robust to input uncertainties.

A RNN model was developed to predict both indoor air temperature (T_{in}) and Empower Wall discharge rate ($Q_{empower}$), the following variables were used as inputs: T_{amb}, $T_{sol,wall,w}$, $T_{sol,wall,n}$, $T_{sol,roof}$, Q_{solar}, Q_{AC}, on/off signals of charging and discharging, charging rate (Q_{charge}), and initial temperature of measured C-C plane temperature ($T_{c\text{-}c\_mea}$ $(t=0)$).

4. MODEL PERFORMANCE COMPARISION AND RESULTS ANALYS

In this section, the results from the above models were compared and analysed. Specifically, the training and test results of the predicted T_{in} from the RC model were compared with those from the RNN model, the training and test results of the predicted $Q_{empower}$ from the regression model were compared with those from the RNN model. The data interval is 1 minute.

4.1 Comparison and analysis of indoor air temperature prediction results

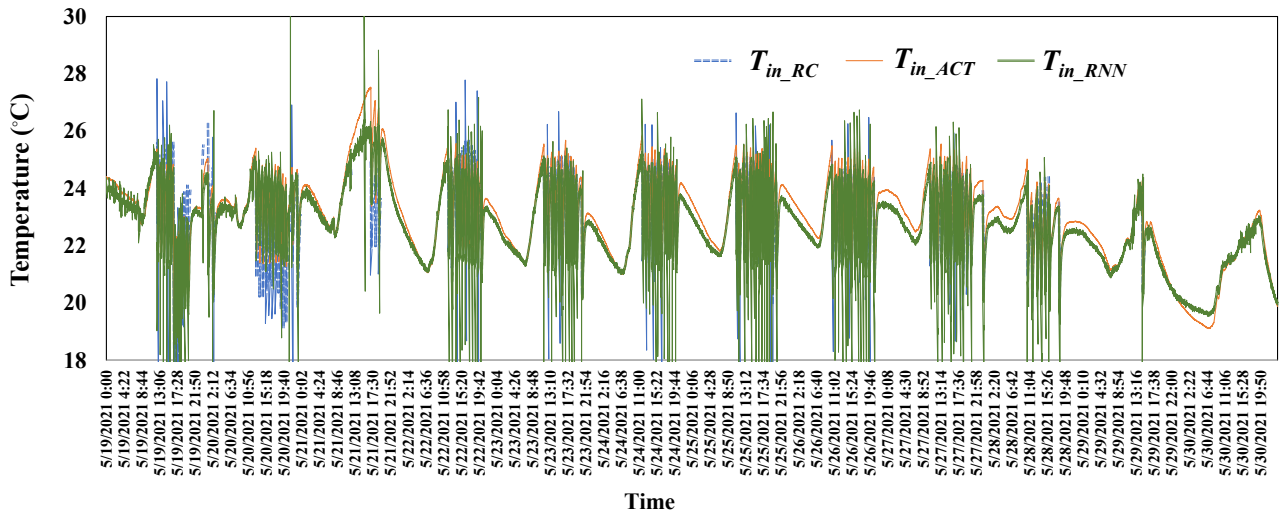

Fig. 5 Training results of indoor air temperature prediction

The indoor air temperature prediction training and test results from both RC model and RNN model were shown in Fig.5 and Fig.6, respectively. Actually, the whole month data in May, 2021 were used as training data for RNN model (to predict both T_{in} and $Q_{empower}$) and the data from May 19 to 30, 2021 were used as the training data for RC model. Such intended approach aimed to introduce more data for RNN model training since machine learning algorithms often require higher amount of data to train the model. On the contrary, due to the physical knowledge introduced into the RC model, it often requires less data for calibration and training [13].

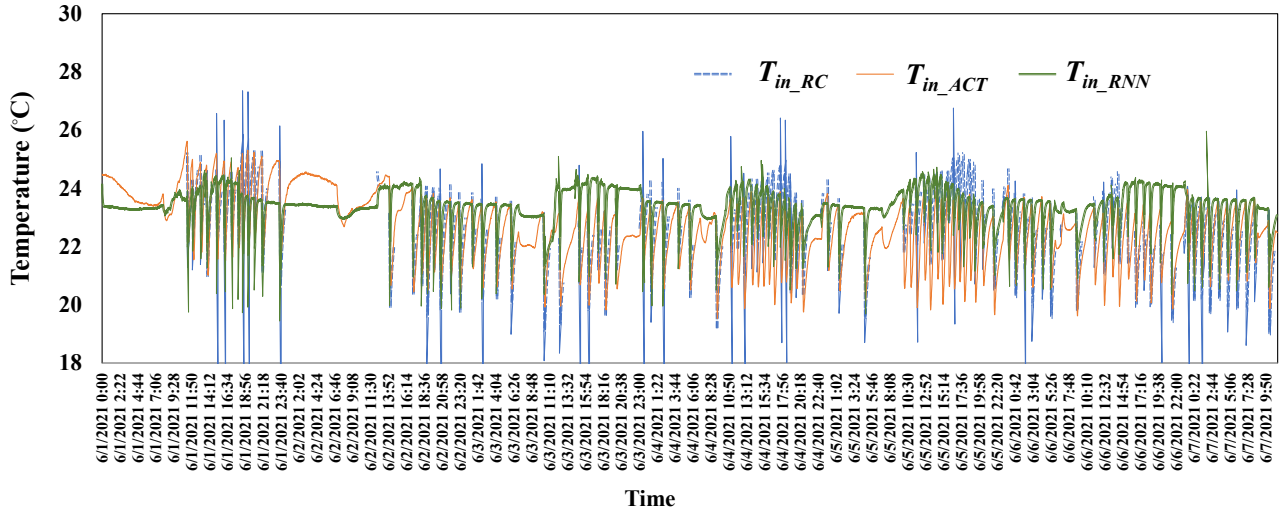

Fig. 6 Test results of indoor air temperature prediction

T_{in_ACT} is the measured mean indoor air temperature, T_{in_RC} is the predicted results from the RC model and T_{in_RNN} is the predicted result from the RNN model, as shown in Fig.5 and 6. The training RMSE values for RC model and RNN model are 0.70 and 0.37 ℃, respectively. However, the test RMSE values for RC model and RNN model are 0.78 and 1.22 ℃, respectively. Such accuracy comparison may suggest that machine learning algorithms may have higher risk of overfitting problem and thanks to the known physical knowledge about the modelled system, gray-box models are more likely to have stable performance.

4.2 Comparison and analysis of discharge rate prediction results

The discharge rate prediction training and test results from both regression model and RNN model were shown in Fig.7 and Fig.8, respectively. $Q_{empower\_ACT}$ is the measured Empower Wall discharge rate, $Q_{empower\_Reg}$ is the predicted results from the regression model and $Q_{empower\_RNN}$ is the predicted result from the RNN model.

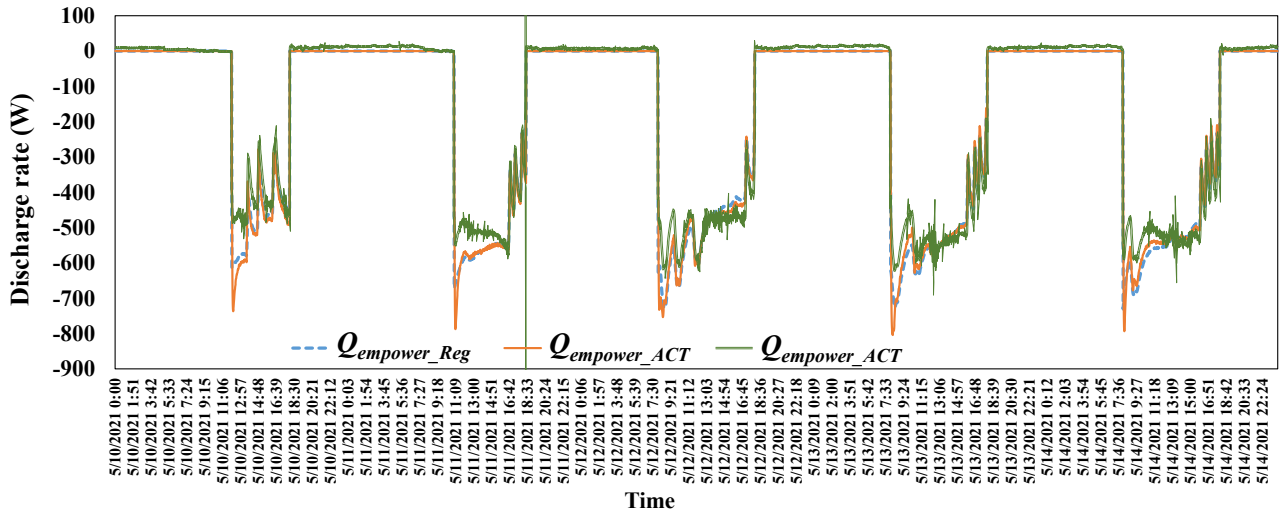

Fig. 7 Training results of Empower Wall discharge rate

In terms of the training results, the accuracy of the RNN model was not much worse than that of the regression model. However, for THE test data, the RNN model can hardly accurately capture the short-term fluctuations during discharging periods which were likely to be caused by the T_{in} fluctuation, in another word, the fluctuation of the difference between T_{in} and $T_{C\text{-}C}$. It seems that further tuning work for RNN model is needed.

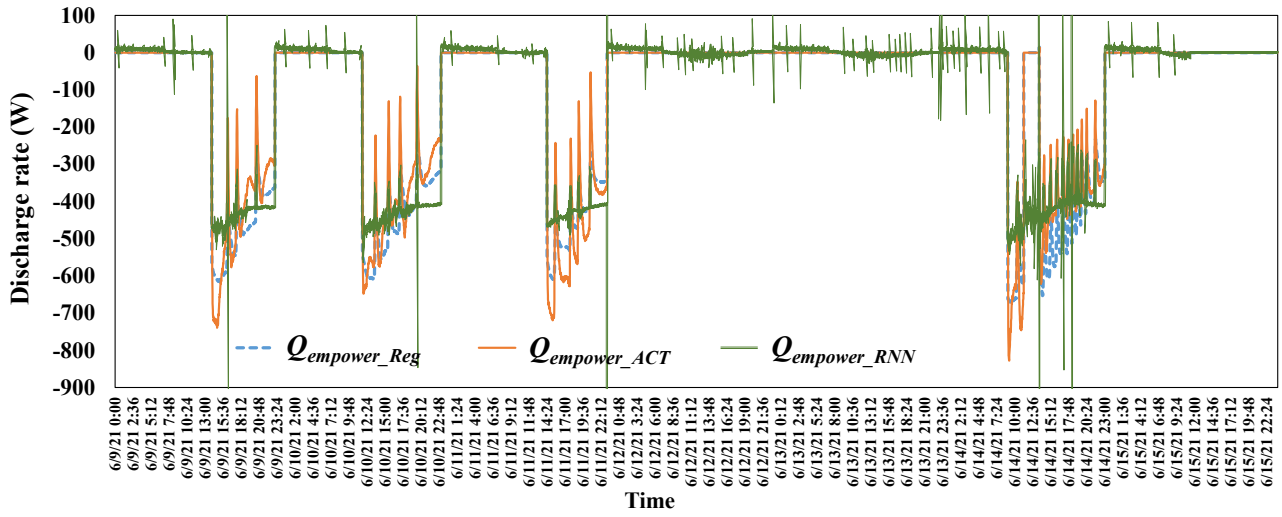

Fig. 8 Test results of Empower Wall discharge rate

5. CONCLUSIONS

An advanced TES+AIS integrated wall system was originally designed to collect and store heating/cooling energy during non-peak load hours so that energy consumption and cost can be reduced. In order to be applied into optimal controls, data-driven models, including gray-box model, simplified statistical (regression) model, and machine learning model were developed to predict both indoor air temperature and discharge rate from the integrated wall system (Empower Wall). The data measured from a real conference room with a RTU air conditioning system, local weather station, and the Empower Wall system were used to train and test the models.

In terms of the indoor air temperature prediction, due to the physical details within the model, the prediction results from the gray-box model (i.e., RC model) were more accurate and more likely to stay reliable, compared to those from the RNN model. The RNN model was not sensitive to the short-term fluctuations for prediction of the discharge rate, compared to the regression model. It is worth noticing that theoretically, $Q_{empower}$ is coupled with the T_{in}. The RNN model predicted both at the same time, while the RC model and regression model took measured $Q_{empower}$ and T_{in} as inputs, respectively. Therefore, to form a fairer comparison, an integrated gray-box/regression model may be required to be developed in the future study.

ACKNOWLEDGMENT

This material is based upon work supported by the US Department of Energy's (DOE's) Office of Federal Energy Management Program (FEMP). This research used resources of Oak Ridge National Laboratory's Building Technologies Research and Integration Center, which is a DOE Office of Science User Facility. This work was funded under DOE FEMP activity no. EL1710000. This manuscript has been authored by UT-Battelle LLC under contract DEAC05-00OR22725 with DOE. The US government retains and the publisher, by accepting the article for publication, acknowledges that the US government retains a nonexclusive, paid-up, irrevocable, worldwide license to publish or reproduce the published form of this manuscript, or allow others to do so, for US government purposes.

NOMENCLATURE

α	solar absorption coefficient	*air*	air
A	area (m^2)	*amb*	ambient air
c	specific heat (J/(kg.K))	*c-c*	c-c panel

C	equivalent overall thermal capacitances (J/K)	charge	charging
C_1 C_2	coefficient (-)	*chiller*	chiller
$Coe_{dis\ 1}$…$Coe_{dis\ 8}$	coefficient (-)	*empower*	empower wall
F	view factor (-)	*in*	indoor air
h	convective heat transger coefficient ()	*im*	internal thermal mass
HFA	heat flux (W/m^2)	*m*	measured
I	direct normal solar irradiance (W/m^2)	*n*	north
Q	Heat gain (W)	*roof*	roof
Q_{solar}	solar radiation through window (W)	*rtn*	return air
R	equivalent overall thermal resistances (K/W)	*sol*	solar
SHGC	Solar heat gain coefficient (-)	*sup*	supply air
T	temperature (°C)	*tot*	total
V	volume flow rate	*w*	west
ρ	density (kg/m^3)	*wa*	water
Subscripts		*wall*	exterior envelope
AC	air conditioning (conditioner)	*win*	windows

REFERENCES

[1] Iffa, E., Hun, D., Salonvaara, M., Shrestha, S. and Lapsa, M., "Performance evaluation of a dynamic wall integrated with active insulation and thermal energy storage systems", *Journal of Energy Storage*, 46, pp.103815, (2022).

[2] Romaní, J., Belusko, M., Alemu, A., Cabeza, L.F., de Gracia, A. and Bruno, F., "Control concepts of a radiant wall working as thermal energy storage for peak load shifting of a heat pump coupled to a PV array", *Renewable energy*, 118, pp. 489-501, (2018).

[3] Cui, B., Dong, J., Lee, S., Im, P., Salonvaara, M., Hun, D. and Shrestha, S., "Model predictive control for active insulation in building envelopes", *Energy and Buildings*, 267, pp.112108 (2022).

[4] Atkins, C., Hun, D., Im, P., Post, B., Slattery, B., Iffa, E., Cui, B., Dong, J., Barnes, A., Vaughan, J. and Roschli, A., "Empower Wall: Active insulation system leveraging additive manufacturing and model predictive control", *Energy Conversion and Management*, 266, pp.115823 (2022).

[5] Jung, S., Yoon, Y., Im, P., Salonvaara, M., Dong, J., Cui, B. and Lapsa, M., "Peak cooling load shift capability of a thermal energy storage system integrated with an active insulation system in US climate zones", *Energy and Buildings*, 277, pp.112484 (2022).

[6] Cui, B., Fan, C., Munk, J., Mao, N., Xiao, F., Dong, J. and Kuruganti, T., "A hybrid building thermal modeling approach for predicting temperatures in typical, detached, two-story houses", *Applied Energy*, 236, pp.101-116 (2019).

[7] Dong, B., Li, Z., Rahman, S.M. and Vega, R., "A hybrid model approach for forecasting future residential electricity consumption", *Energy and Buildings*, 117, pp.341-351 (2016).

[8] Belić, F., Hocenski, Ž. and Slišković, D., "Thermal modeling of buildings with RC method and parameter estimation", *In 2016 International Conference on Smart Systems and Technologies*, pp. 19-25, (2016).

[9] Kim, D., Cai, J., Ariyur, K.B. and Braun, J.E., "System identification for building thermal systems under the presence of unmeasured disturbances in closed loop operation: Lumped disturbance modeling approach", *Building and Environment*, 107, pp.169-180, (2016).

[10] Braun, J.E. and Chaturvedi, N., "An inverse gray-box model for transient building load prediction", *HVAC&R Research*, 8(1), pp.73-99, (2002).

[11] Kusiak, A., Li, M. and Tang, F., "Modeling and optimization of HVAC energy consumption", *Applied Energy*, 87(10), pp.3092-3102, (2010).

[12] Rahman, A., Smith, A.D., "Predicting heating demand and sizing a stratified thermal storage tank using deep learning algorithms", *Applied Energy*, 228, pp.108-121, (2018).

[13] Afroz, Z., Shafiullah, G.M., Urmee, T. and Higgins, G., "Modeling techniques used in building HVAC control systems: A review", *Renewable and sustainable energy reviews*, 83, pp.64-84, (2018).